Available online at www.sciencedirect.com
SCIENCE DIRECT®
PERGAMON
Polyhedron 22 (2003) 2639–2646
POLYHEDRON
www.elsevier.com/locate/poly

Optically active transition metal complexes. Part 133[1]. Preparation, epimerization and crystallization of chiral-at-metal rhodium(III) half-sandwich complexes

Henri Brunner [a,*], A. Köllnberger [a], Manfred Zabel [b]

[a] Institut für Anorganische Chemie, Universität Regensburg, D-93040 Regensburg, Germany
[b] Zentrale Analytik, Röntgenstrukturanalyse, Universität Regensburg, D-93040 Regensburg, Germany

Received 13 March 2003; accepted 12 May 2003

Abstract

The complexes Cp*Rh(beapy)Cl (**5**) and Cp*Ir(beapy)Cl (**6**) were synthesized by reaction of $[Cp^*MCl_2]_2$ (M = Rh, Ir) and the deprotonated ligand Hbeapy, the condensation product of benzylamine and 2-pyrrolcarbaldehyde. In each case two enantiomers (S_M) and (R_M) arise, differing only in the metal chirality. The CH_2 group of the benzyl substituent in the ligand forms an AB spectrum which was used for ^1H NMR coalescence measurements ($T_c = 115.1$ °C). The half-life for the racemization of Cp*Rh(beapy)Cl (**5**) was 46 ms at 115.1 °C. Substitution of the chloride ligand in Cp*Rh(pepy)Cl (**3**), pepy anion of Schiff base (+)-2-*N*-[(*S*)-1-phenylethyl]pyrrolcarbaldimine, afforded the complexes Cp*Rh(pepy)Br (**7**) and Cp*Rh(pepy)I (**8**). Single crystals of the two compounds contained only one of the two diastereomers. In solution the compounds epimerized via a change of the metal configuration, the half-life for (R_{Rh},S_C)-Cp*Rh(NN*)I (**8**) being 40.8 min at −40 °C in CD_2Cl_2 solution (obtained by time dependent integration of suitable ^1H NMR signals). Reaction of $[CpRhCl_2]_2$ with (+)-*N*-[(*S*)-1-phenylethyl]salicylaldimine gave CpRh(pesa)Cl (**9**). Surprisingly, single crystals of **9** contained both diastereomers (R_{Rh},S_C) and (S_{Rh},S_C) in a 1:1 ratio following the molecular recognition motif of the inverted pianostools. The half-lifes for the epimerization of **9** with respect to the metal center, derived from ^1H NMR coalescence experiments, were 31 and 9.2 ms at 11.3 °C (CD_2Cl_2) for the forward and back reactions, respectively.

Keywords: Chiral-at-metal complexes; Rhodium; Configurational stability; Epimerization; X-ray structure analyses

1. Introduction

Most of the organometallic chiral-at-metal compounds are half-sandwich complexes [1–3]. A frequent ligand combination of this type in the chemistry of rhodium and iridium is a cyclopentadienyl or pentamethylcyclopentadienyl ligand, a halide ligand and an unsymmetrical anionic chelate ligand with a chiral carbon atom, e.g. of (*S*)-configuration. Such a ligand combination gives rise to two diastereomers (R_M,S_C) and (S_M,S_C) which differ only in the metal configuration. In these Rh and Ir compounds the configuration at the metal center often is labile [4–9]. Therefore, such complexes epimerize in solution via a change of the metal configuration. Occasionally, this aspect has been overlooked and wrong conclusions have been drawn. In 1997 Loza et al. published the rhodium complex Cp*Rh(pesa)Cl (**1**) formed in the reaction of (+)-*N*-[(*S*)-1-phenylethyl]salicylaldimine (Hpesa) and $[Cp^*RhCl_2]_2$ [10]. In the crystal of Cp*Rh(pesa)Cl only the (R_{Rh},S_C)-diastereomer was present. As in the ^1H NMR spectrum at RT only one set of broad signals was observed, it was assigned to the (R_{Rh},S_C)-diastereomer claiming a high diastereomeric excess [10]. In a VT NMR study of Cp*Rh(pesa)Cl (**1**) we could show that at RT the signals of the diastereomers (R_{Rh},S_C) and (S_{Rh},S_C) coalesced, whereas at low temperatures they

* Corresponding author. Tel.: +49-941-943-4440; fax: +49-941-943-4439.
E-mail address: henri.brunner@chemie.uni-regensburg.de (H. Brunner).
[1] Part 132. H. Brunner, M. Weber, M. Zabel, T. Zwack, Angew. Chem., in press; Anbew. Chem. Int. Ed. in press.

0277-5387/03/$ - see front matter © 2003 Elsevier Ltd. All rights reserved.
doi:10.1016/S0277-5387(03)00346-2

were well resolved indicating a high configurational instability at the metal atom (half-lifes for the interconversion of the two diastereomers 28 and 6.7 ms at 21 °C for Cp*Rh(pesa)Cl (**1**) and 50 and 8 ms at −1.8 °C for Cp*Ir(pesa)Cl (**2**) [4,11] (Scheme 1).

In the complexes Cp*Rh(pepy)Cl (**3**) and Cp*Ir(pepy)Cl (**4**), derived from ligand (+)-2-*N*-[(*S*)-1-phenylethyl]pyrrolcarbaldimine (Hpepy), the configuration at the metal center proved to be labile, too, although the half-lifes for approach to equilibrium were much longer (19.4 min for Cp*Rh(pepy) (**3**) and 30.6 min for Cp*Ir(pepy)Cl (**4**) at −50 °C [4]).

In the present paper we describe (i) the synthesis of the complexes Cp*M(beapy)Cl, M = Rh (**5**) and Ir (**6**), derived from the achiral ligand Hbeapy, the diastereotopic benzyl protons of which provided information on the stability of the metal configuration in coalescence experiments, (ii) the synthesis of the complexes Cp*Rh(pepy)Hal, Hal = Br (**7**), I (**8**) to investigate the influence of the halide ligand on the half-lifes of the epimerization reactions and the diastereomer concentrations at equilibrium, and (iii) the synthesis of CpRh(pesa)Cl (**9**), the Cp analogue of **1**, one of the rare cases in which two diastereomers co-crystallized in a 1:1 ratio in the same single crystal [11].

2. Experimental

2.1. Physical measurements

^{1}H NMR spectra: Bruker AC 250 (250 MHz) and ARX 400 (400 MHz); TMS as internal standard. MS: Finnigan MAT 95 and Finnigan MAT 311A. The most intense peak was specified. Elemental analyses: Elementar Vario EL III. Melting points: Büchi SMP 20. Polarimetric measurements: Perkin–Elmer polarimeter 241.

2.2. Ligands and precursors

The ligands 2-*N*-benzylpyrrolcarbaldimine (Hbeapy) [12], (+)-2-*N*-[(*S*)-1-phenylethyl]pyrrolcarbaldimine (Hpepy) [13], (+)-2-*N*-[(*S*)-1-phenylethyl]salicylaldimine (Hpesa) [14] and the precursors $[Cp^*MCl_2]_2$ and $[CpMCl_2]_2$, M = Rh, Ir [15] were synthesized by published methods.

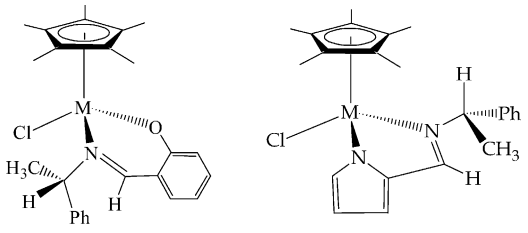

Cp*Rh(pesa)Cl (**1**) Cp*Rh(pepy)Cl (**3**)
Cp*Ir(pesa)Cl (**2**) Cp*Ir(pepy)Cl (**4**)

Scheme 1. Complexes **1**–**4** (only the (R_M,S_C)-diastereomers shown).

2.3. Cp*Rh(beapy)Cl (5) and Cp*Ir(beapy)Cl (6)

Hbeapy (180 mg, 0.97 mmol) was deprotonated with 109 mg (1.36 mmol) of KO^{t}Bu in 30 ml of CH_2Cl_2 under N_2. After stirring for 1 h at RT 0.97 mmol of $[Cp^*RhCl_2]_2$ (300 mg) or $[Cp^*IrCl_2]_2$ (386 mg) were added. After stirring for 20 h at RT the solvent was removed. The residue was dissolved in 20 ml of toluene and filtered over celite®. For crystallization petroleum ether was added to the filtrate.

2.3.1. Cp*Rh(beapy)Cl (5)

Orange powder. Yield: 367 mg, 82%. M.p. (dec.) > 200 °C. ^{1}H NMR (250 MHz, 297 K, $CDCl_3$): δ = 7.41–7.34 (m, 6H, Ph, NC*H*), 7.13 (s, 1H, pyrr-H^5), 6.55 (dd, ^3J = 3.8 Hz, ^4J = 1.0 Hz, 1H, pyrr-$H^{3/4}$), 6.28 (dd, ^3J = 3.8 Hz, ^4J = 1.7 Hz, 1H, pyrr-$H^{3/4}$), 5.08 (dd, ^2J = 17.5 Hz, ^4J = 0.9 Hz, 1H, CH_AH$_B$), 5.04 (dd, ^2J = 17.5 Hz, ^4J = 0.9 Hz, 1H, CH$_A$$H_B$), 1.74 (s, 15H, C_5Me_5). FAB-PI-LSIMS (CH_2Cl_2): *m*/*z* = 456 (M, 40), 421 (M–Cl, 100). $C_{22}H_{26}ClN_2Rh$ (456.8): Calc. C 57.84, H 5.74, N 6.13; Found: C 58.06, H 6.21, N 5.94%.

2.3.2. Cp*Ir(beapy)Cl (6)

Red–orange powder. Yield: 420 mg, 79%. M.p. (dec.) > 200 °C. ^{1}H NMR (250 MHz, 297 K, $CDCl_3$): δ = 7.44–7.12 (m, 7H, Ph, pyrr-H^5, NC*H*), 6.58 (dd, ^3J = 3.8 Hz, ^4J = 1.1 Hz, 1H, pyrr-$H^{3/4}$), 6.30 (dd, ^3J = 3.8 Hz, ^4J = 1.7 Hz, 1H, pyrr-$H^{3/4}$), 5.10 (dd, ^2J = 15.7 Hz, ^4J = 1.4 Hz, 1H, CH_AH$_B$), 5.02 (dd, ^2J = 15.7 Hz, ^4J = 1.4 Hz, 1H, CH$_A$$H_B$), 1.72 (s, 15H, C_5Me_5). FAB-PI-LSIMS (CH_2Cl_2): *m*/*z* = 546 (M, 68), 411 (M–Cl, 100). $C_{22}H_{26}ClN_2Ir$ (546.1): Calc. C 48.38, H 4.80, N 5.13; Found: C 48.65, H 5.03, N 4.89%.

2.4. Cp*Rh(pepy)Br (7) and Cp*Rh(pepy)I (8)

Cp*Rh(pepy)Cl (**3**) (70.6 mg, 0.15 mmol) was dissolved in 15 ml of absolute methanol under N_2. A tenfold amount of NaBr (154.4 mg, 1.5 mmol) or NaI (224.8 mg, 1.5 mmol) was added. After stirring for 1 h at RT, the solvent was removed. The residue was dissolved in 10 ml of CH_2Cl_2 and the salts were removed by filtration over celite®. To complete the halide exchange, this procedure was repeated another two times. After the last exchange process, the solvent was removed to give the product as a red powder.

2.4.1. Cp*Rh(pepy)Br (7)

Red powder. Yield: 75.6 mg, 98%. M.p. (dec.) > 170 °C. ^{1}H NMR (400 MHz, $CDCl_3$) of the (R_{Rh},S_C)-diastereomer, (S_{Rh},S_C)-diastereomer in brack-

ets: $\delta = 7.66$–7.09 (m, 7H, N=C*H*, pyrr-H^5, Ph), 6.55 [6.57] (dd, $^3J = 3.7$ Hz, $J = 1.1$ Hz, 1H, pyrr-H^4), 6.26 (ddd, $^3J = 3.7$ Hz, $J = 1.8$ Hz, $J = 0.3$ Hz, 1H, pyrr-H^3), 5.27 (q, $^3J = 7.0$ Hz, 1H, CH_3CHPh), 1.77 [1.83] (d, $^3J = 7.0$ Hz, 3H, CH_3CHPh), 1.66 [1.71] (s, 15H, C_5Me_5). FAB-PI-LSIMS (CH_2Cl_2): $m/z = 516$ (M, 8), 435 (M–Br, 100). $C_{23}H_{28}BrN_2Rh$ (514.3): Calc. C 53.61, H 5.48, N 5.46; Found: C 51.85, H 5.48, N 5.37%.

2.4.2. Cp*Rh(pepy)I (**8**)

Red powder. Yield: 81.7 mg, 97%. M.p. (dec.) > 145 °C. ^{1}H NMR (400 MHz, $CDCl_3$) of the (R_{Rh},S_C)-diastereomer, (S_{Rh},S_C)-diastereomer in brackets: $\delta = 7.57$–7.10 (m, 7H, N=C*H*, pyrr-H^5, Ph), 6.62 (dd, $^3J = 3.8$ Hz, $J = 1.1$ Hz, 1H, pyrr-H^4), 6.27 [6.25] (ddd, $^3J = 3.8$ Hz, $J = 1.8$ Hz, $J = 0.4$ Hz, 1H, pyrr-H^3), 5.22 [5.13] (q, $^3J = 7.0$ Hz, 1H, CH_3CHPh), 1.79 [1.83] (d, $^3J = 7.0$ Hz, 3H, CH_3CHPh), 1.72 [1.81] (s, 15 H, C_5Me_5). FAB-PI-LSIMS (CH_2Cl_2): $m/z = 563$ (M, 10), 435 (M–I, 100). $C_{23}H_{28}IN_2Rh$ (561.3): Calc. C 49.13, H 5.02, N 4.98; Found: C 48.35, H 4.98, N 4.74%.

2.5. CpRh(pesa)Cl (**9**)

(*S*)-Hpesa (225 mg, 1.0 mmol) was deprotonated with 112 mg (1.0 mmol) of KO^{t}Bu in 10 ml of abs. CH_2Cl_2. After 1 h $[CpRhCl_2]_2$ (100 mg, 0.27 mmol) was added at 0 °C. The solution was stirred for 4 h at RT and then filtered over celite®. After removing the solvent the residue was washed with pentane. For crystallization the residue was dissolved in toluene with petroleum ether slowly diffusing into the toluene solution.

Red powder. Yield: 137 mg, 60%. M.p. (dec.) $>$ 200 °C. ^{1}H NMR (400 MHz, 213 K, CD_2Cl_2) of the major diastereomer, minor diastereomer in brackets: $\delta = 8.09$ [7.81] (s, 1H, NC*H*), 7.55–7.08 (m, 7H, Ph, sal-H), 6.89 [6.80] (d, $^3J = 8.0$ Hz, 1H, sal-H), 6.55 [6.44] (ddd, $^3J = 8.0$ Hz, $^3J = 8.0$ Hz, $^4J = 1.1$ Hz, 1H, sal-H), 5.80 [5.33] (q, $^3J = 7.0$ Hz, 1H, CH_3CHPh), 5.00 [5.27] (s, 5H, C_5H_5); 1.74 [1.89] (d, $^3J = 7.0$ Hz, 3H, CH_3CHPh). FAB-PI-LSIMS (CH_2Cl_2): $m/z = 427$ (M, 32), 392 (M–Cl, 100). $C_{20}H_{19}ClNOP$ (427.7): Calc. C 56.16, H 4.48, N 3.27; Found: C 57.96, H 4.90, N 3.30%.

2.6. X-ray crystallography

Diffraction data were collected on a STOE-IPDS using Mo Kα radiation ($\lambda = 0.7107$ Å). Crystal data and details of the structure determination are shown in Table 1. The structures were solved by direct methods (SIR-97 [16]). They were refined on F^2 by the full-matrix least-squares technique (SHELXL-97 [17]). For all compounds, where the absorption coefficient was greater than 1.0 mm^{-1}, numerical absorption correction from crystal shape was applied. All hydrogen atoms for 'beapy-compounds' were calculated geometrically and a riding model was used during the refinement process. For the 'pesa-compound' all H-atoms were located by difference Fourier synthesis and refined isotropically, and for the 'pepy-compounds' a mixture of both methods was used.

3. Cp*Rh(beapy)Cl (5) and Cp*Ir(beapy)Cl (6)

3.1. Synthesis and X-ray structure analyses

Condensation of benzylamine and 2-pyrrolcarbaldehyde in methanol gave ligand Hbeapy. Hbeapy was deprotonated with KO^{t}Bu in CH_2Cl_2 and reacted with the organometallic precursors $[Cp^*RhCl_2]_2$ and $[Cp^*IrCl_2]_2$ (Scheme 2). The two enantiomers of the neutral complexes (R_{Rh})-Cp*Rh(beapy)Cl (R_{Rh})-(**5**) and (S_{Rh})-Cp*Rh(beapy)Cl (S_{Rh})-(**5**) as well as (R_{Ir})-Cp*Ir(beapy)Cl (R_{Ir})-(**6**) and (S_{Ir})-Cp*Ir(beapy)Cl (S_{Ir})-(**6**) were formed differing only in the metal configuration.

Single crystals of Cp*Rh(beapy)Cl (**5**) and Cp*Ir(beapy)Cl (**6**) were obtained by slow diffusion of petroleum ether into a toluene solution of the complexes at RT. Fig. 1 shows the crystal structure of Cp*Rh(beapy)Cl (**5**). For the specification of the metal configuration the ligand priority sequence Cp > Cl > N(imine) > N(pyrrole) was used [18,19]. There is a center of inversion between the two enantiomers (R_{Rh})-Cp*Rh(beapy)Cl and (S_{Rh})-Cp*Rh(beapy)Cl.

The iridium compound Cp*Ir(beapy)Cl (**6**) crystallized analogously. Table 1 contains the crystallographic data and Table 2 the most important bond lengths, bond angles and dihedral angles of **5** and **6**.

3.2. Enantiomer interconversion

At 297 K the CH_2 group of the benzyl substituent in Cp*Rh(beapy)Cl (**5**) showed two strongly coupling doublets at 5.08 and 5.04 ppm indicating an AB spectrum of two geminal protons. Increasing the temperature the signals of the two protons coalesced forming a horizontal connection at the coalescence temperature $T_c = 115.1$ °C. At temperatures of 413 K there was only one sharp signal for the CH_2 protons. The process underlying the coalescence is a rapid interconversion of the enantiomers of **5** which make the diastereotopic protons of the benzyl group identical on the NMR time scale. An evaluation of the coalescence measurement by published methods [21] gave a half-life of 46 ms at 115.1 °C for Cp*Rh(beapy)Cl (**5**). The parameters of the measurement are summarized in Table 4. Coalescence studies with Cp*Ir(beapy)Cl (**6**) were not possible because decomposition started at temperatures above 50 °C.

Table 1
Crystallographic data of complexes **5**–**9**

Compound	Cp*Rh(beapy)Cl (**5**)	Cp*Ir(beapy)Cl (**6**)	Cp*Rh(pepy)Br (**7**)	Cp*Rh(pepy)I (**8**)	CpRh(pesa)Cl (**9**)
Empirical formula	$C_{22}H_{26}ClN_2Rh$	$C_{22}H_{26}ClIrN_2$	$C_{23}H_{28}BrN_2Rh$	$C_{23}H_{28}IN_2Rh$	$C_{20}H_{19}ClNORh$
Formula weight	456.81	546.12	515.28	562.28	427.72
Crystal size (mm × mm × mm)	0.58 × 0.14 × 0.06	0.60 × 0.38 × 0.36	0.24 × 0.10 × 0.06	0.60 × 0.16 × 0.10	0.31 × 0.12 × 0.06
Crystal color, habit	red rod	orange prism	red prism	red rod	brown prism
Crystal system	orthorhombic	orthorhombic	orthorhombic	orthorhombic	monoclinic
Space group	*Pccn*	*Pccn*	$P2_12_12_1$	$P2_12_12_1$	$P2_1$
Unit cell dimensions					
a (Å)	7.7632(4)	7.8444(3)	7.6165(4)	7.6843(4)	12.3696(13)
b (Å)	21.8151(13)	21.7956(11)	11.2156(6)	11.1852(6)	10.5226(9)
c (Å)	26.6522(13)	26.3499(17)	24.9561(15)	25.650(2)	14.7016(17)
α (°)	90	90	90	90	90
β (°)	90	90	90	90	111.677(12)
γ (°)	90	90	90	90	90
V (Å^3)	4513.7(4)	4505.1(4)	2131.84(17)	2204.6(2)	1778.2(3)
Z	8	8	4	4	4
D_{calc} (g cm^{-3})	1.344	1.610	1.605	1.694	1.598
F (0 0 0)	1872	2128	1040	1112	864
Absorption coefficient (mm^{-1})	0.88	6.05	2.69	2.18	1.12
Data collection					
T (K)	173(1)	173(1)	173(1)	173(1)	297(2)
θ Range for data collection (°)	2.48–25.83	2.43–25.79	2.44–25.77	2.42–25.73	1.85–25.84
Index ranges	$-9 \le h \le 8$, $-26 \le k \le 26$, $-32 \le l \le 32$	$-8 \le h \le 8$, $-26 \le k \le 26$, $-32 \le l \le 32$	$-9 \le h \le 9$, $-13 \le k \le 13$, $-30 \le l \le 30$	$-9 \le h \le 8$, $-13 \le k \le 13$, $-31 \le l \le 31$	$-15 \le h \le 15$, $-12 \le k \le 12$, $-18 \le l \le 17$
Reflections collected	34 559	59 960	27 987	17 360	21 761
Independent reflections	4333	4122	4068	4170	6770
Observed reflections [$I > 2\sigma(I)$]	2824	3871	3733	3998	4866
R_{int}	0.0807	0.0579	0.0579	0.0403	0.0714
Refinement					
Hydrogen treatment	constr.	constr.	mixed	mixed	constr.
Data, restraints, parameters	4333, 0, 235	4122, 0, 235	4068, 0, 264	4289, 0, 378	6770, 1, 433
Goodness-of-fit on F^2	0.943	1.224	0.997	1.042	0.894
Final R indices [$I > 2\sigma(I)$]	$R_1 = 0.0349$, $wR_2 = 0.0622$	$R_1 = 0.0310$, $wR_2 = 0.0769$	$R_1 = 0.0220$, $wR_2 = 0.0480$	$R_1 = 0.0184$, $wR_2 = 0.0457$	$R_1 = 0.0392$, $wR_2 = 0.0761$
R indices (all data)	$R_1 = 0.0838$, $wR_2 = 0.0744$	$R_1 = 0.0350$, $wR_2 = 0.0789$	$R_1 = 0.0258$, $wR_2 = 0.0488$	$R_1 = 0.0195$, $wR_2 = 0.0461$	$R_1 = 0.0631$, $wR_2 = 0.0812$
Absolute structure parameter			−0.01(1)	−0.03(2)	0.01(4)
Largest peak, hole (e Å^{-3})	0.755 and −0.334	1.233 and −0.522	0.529 and −0.240	0.719 and −0.326	0.795 and −0.276
CCDC number	202467	202468	202465	202464	202466

4. Cp*Rh(pepy)Br (7) and Cp*Rh(pepy)I (8)

4.1. Synthesis and X-ray structure analyses

The complexes Cp*Rh(pepy)Br (**7**) and Cp*Rh(pepy)I (**8**) were synthesized by halogen exchange reactions starting from Cp*Rh(pepy)Cl (**3**) [4] (Scheme 3). For these substitutions Cp*Rh(pepy)Cl (**3**) was dissolved in methanol and a tenfold excess of NaBr or NaI was added. After a short time the reaction mixture was at equilibrium. By removing the solvent, dissolving the residue in CH_2Cl_2 and filtering over celite® the product was isolated. For a halide exchange of 99.9% the process must be repeated another two times. As the ^{1}H NMR signals of the products differ from those of the starting material, the progress of the reaction can be monitored by ^{1}H NMR spectroscopy.

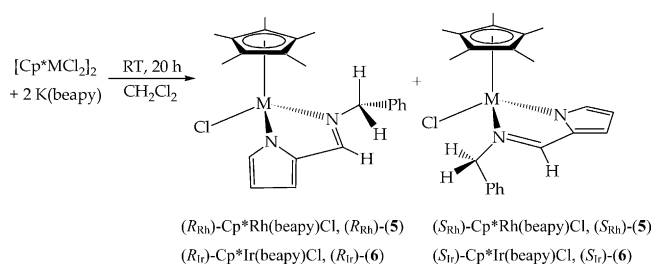

Scheme 2. Complexes **5** and **6**.

Cp*Rh(pepy)Br (**7**) and Cp*Rh(pepy)I (**8**) form two diastereomers (R_{Rh},S_C)- and (S_{Rh},S_C)-Cp*Rh(pepy)Br and (R_{Rh},S_C)- and (S_{Rh},S_C)-Cp*Rh(pepy)I differing only in the metal configuration. In CD_2Cl_2 solution at room temperature the equilibrium concentrations are (R_{Rh},S_C):(S_{Rh},S_C) = 87:13 both for Cp*Rh(pepy)Br (**7**) and Cp*Rh(pepy)I (**8**).

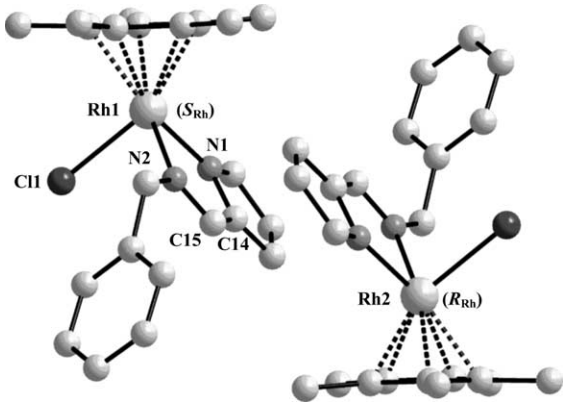

Fig. 1. Crystal structure of Cp*Rh(beapy)Cl (**5**).

Slow diffusion of petroleum ether into toluene solutions of Cp*Rh(pepy)Br (**7**) and Cp*Rh(pepy)I (**8**) afforded single crystals suitable for X-ray structure analyses. Only the (R_{Rh},S_C)-diastereomers of Cp*Rh(pepy)Br (**7**) and Cp*Rh(pepy)I (**8**) crystallized. Scheme 4 shows the crystal structure of (R_{Rh},S_C)-Cp*Rh(pepy)Br (**7**). The structure of (R_{Rh},S_C)-Cp*Rh(pepy)I (**8**) is very similar.

Table 1 contains the crystallographic data and Table 2 representative molecular parameters of the crystal structures of (R_{Rh},S_C)-Cp*Rh(pepy)Br (**7**) and (R_{Rh},S_C)-Cp*Rh(pepy)I (**8**).

4.2. Epimerization studies

Powdered crystals of (R_{Rh},S_C)-Cp*Rh(pepy)I (**8**) were dissolved in CD_2Cl_2 at −80 °C. Due to the time necessary for dissolution and preparing the first measurement at −40 °C, the ^{1}H NMR spectrum taken at $t = 0$ min showed not only the signals of the (R_{Rh},S_C)-diastereomer but also those of the (S_{Rh},S_C)-diastereomer. During the measurement at −40 °C the signals of diastereomer (S_{Rh},S_C)-Cp*Rh(pepy)I increased up to 13% (Scheme 5). The equilibrium concentration was

Table 2
Selected bond lengths (Å), bond angles (°) and dihedral angles (°) of complexes **5**–**8**

	rac-Cp*Rh(beapy)Cl (**5**)	*rac*-Cp*Ir(beapy)Cl (**6**)	Cp*Rh(pepy)Br (**7**)	Cp*Rh(pepy)I (**8**)
Bond lengths				
M1–Cp	1.779	1.779	1.795	1.795
M1–N1	2.064(3)	2.060(4)	2.075(2)	2.079(2)
M1–N2	2.111(3)	2.100(4)	2.151(2)	2.139(2)
M1–Hal1	2.4083(11)	2.4083(13)	2.5396(4)	2.7016(4)
Bond angles				
N1–M1–N2	77.25(13)	76.29(14)	77.44(9)	77.61(9)
N2–M1–Hal1	85.23(9)	83.34(11)	86.19(6)	87.77(6)
Hal1–M1–N1	89.88(9)	87.77(11)	90.04(6)	89.92(6)
Dihedral angles				
M1–N1–C14–C15	1.0(5)	1.9(5)	8.8(3)	6.3(3)
N1–C14–C15–N2	−2.1(6)	−2.0(6)	−6.1(4)	−4.3(4)
C14–C15–N2–M1	2.1(5)	1.1(6)	0.3(4)	0.1(4)
C15–N2–M1–N1	−1.2(3)	0.0(3)	3.3(2)	2.5(2)

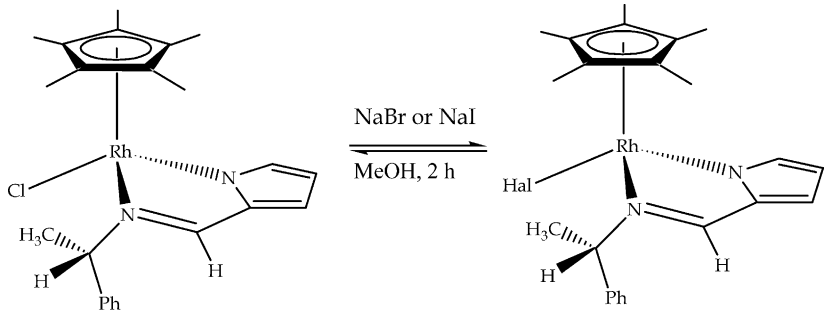

Cp*Rh(pepy)Cl (**3**)

Cp*Rh(pepy)Br (**7**)
Cp*Rh(pepy)I (**8**)

Scheme 3. Halide exchange in Cp*Rh(pepy)Cl (**3**) (only one diastereomer shown).

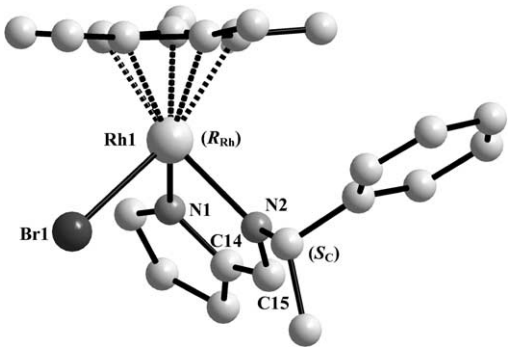

Scheme 4. Crystal structure of (R_{Rh},S_C)-Cp*Rh(pepy)Br (**7**).

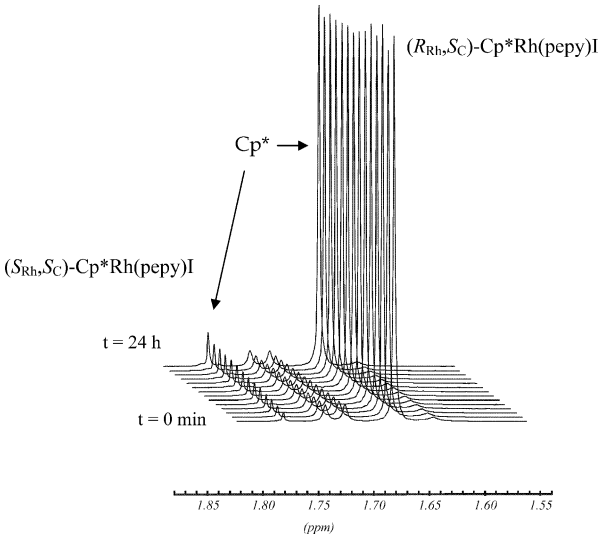

Scheme 5. Time dependent ^{1}H NMR spectra of Cp*Rh(pepy)I (**8**) (233 K, 400 MHz, CD_2Cl_2).

determined after thermostating the sample at −40 °C for 24 h.

Time dependent integration of the Cp*-signals at 1.68 and 1.72 ppm and treatment of the data according to first-order led to the half-life for the approach to the epimerization equilibrium (Scheme 6). This half-life for (R_{Rh},S_C)-Cp*Rh(pepy)I (**8**) at 233 K in CD_2Cl_2 is 40.8 min compared to 2.7 min for (R_{Rh},S_C)-Cp*Rh(pepy)Cl (**1**) at 237 K in CD_2Cl_2 [4]. Thus, in going from the chloro complex **1** to the corresponding iodo complex **8** the configurational stability of the metal atom increases.

5. CpRh(pesa)Cl (9)

5.1. Synthesis and X-ray structure analysis

For the synthesis of CpRh(pesa)Cl (**9**), the Cp analogue of Cp*Rh(pesa)Cl (**1**) [4,10], $[CpRhCl_2]_2$ was added to the deprotonated pesa ligand in CH_2Cl_2 at 0 °C (Scheme 7). Again, two diastereomers (R_{Rh},S_C)- and (S_{Rh},S_C)-CpRh(pesa)Cl (**9**) arise. However, the ^{1}H NMR spectrum at RT showed only one set of broad signals (see below).

Slow diffusion of petroleum ether into a toluene solution of CpRh(pesa)Cl (**9**) at RT gave crystals suitable for X-ray structure analysis. Surprisingly, the two diastereomers (R_{Rh},S_C)- and (S_{Rh},S_C)-CpRh(pesa)Cl (**9**) were present in a 1:1 ratio in the same single crystal. Thus, the two diastereomers of compound **9** follow the molecular recognition motif of the inverted pianostools [20]. There is an 'almost inversion center' between the two diastereomers (R_{Rh},S_C) and (S_{Rh},S_C),

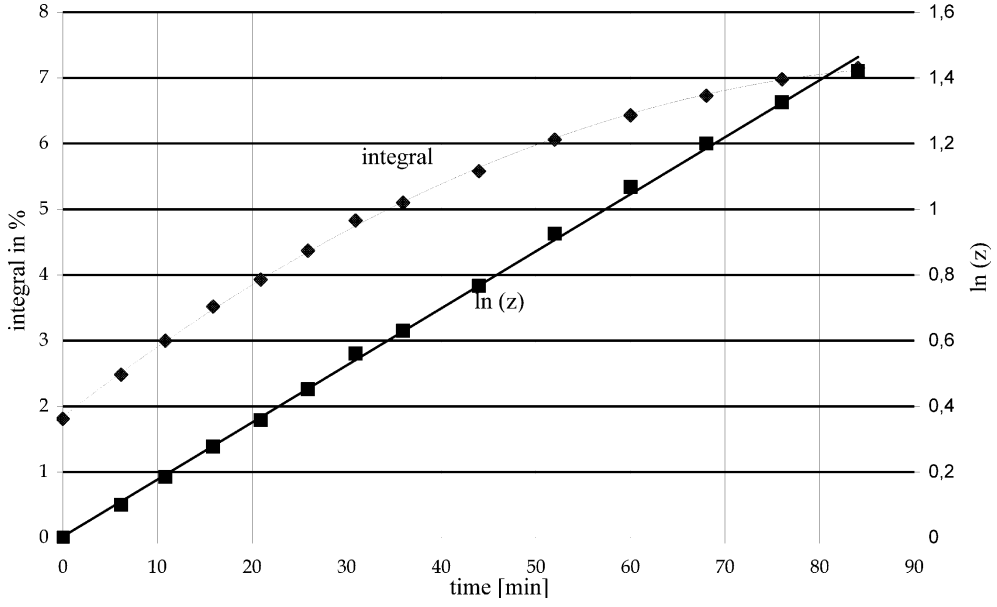

Scheme 6. Kinetics of the epimerization of (R_{Rh},S_C)-Cp*Rh(pepy)I (**8**) (233 K, CD_2Cl_2). Ordinate:integral minor (S_{Rh},S_C)-diastereomer.

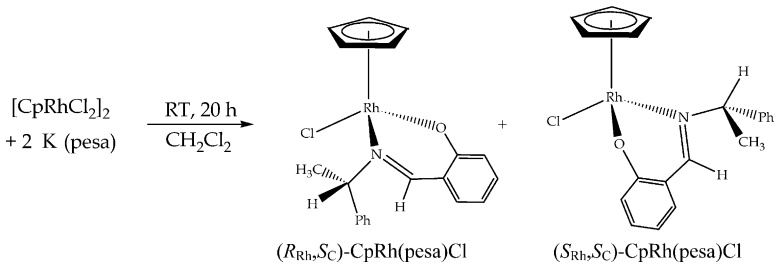

Scheme 7. Synthesis of CpRh(pesa)Cl (**9**).

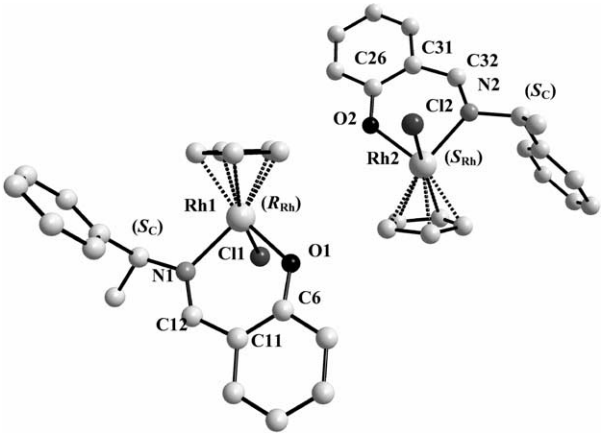

Scheme 8. Crystal structure of CpRh(pesa)Cl (**9**).

which approach each other with their 'racemic sides' forming hydrogen bridges between C–H bonds of the Cp ring and the oxygen and chlorine atoms of the neighbor molecule. The two (S_C)-configurated *N*-substituents which disturb centrosymmetry are oriented to the outside of the inversion pairs. With 5.487 Å the distance between the two rhodium atoms is typical for the molecular recognition motif of the inverted pianostools. The crystal lattice of CpRh(pesa)Cl (**9**) is formed by translation of the inversion pairs of Scheme 8.

Table 1 contains the crystallographic data and Table 3 the most important distances and angles of the two diastereomers of CpRh(pesa)Cl (**9**).

Table 3
Selected bond lengths (Å), bond angles (°) and dihedral angles (°) of complex **9**

	(R_{Rh},S_C)-CpRh-(pesa)Cl (**9**)	(S_{Rh},S_C)-CpRh-(pesa)Cl (**9**)
Bond lengths		
Rh1/2–Cp1/Cp2	1.795	1.802
Rh1/2–N1/2	2.083(5)	2.103(6)
Rh1/2–O1/2	2.046(5)	2.046(5)
Rh1/2–Cl1/2	2.409(2)	2.406(9)
Bond angles		
N1/2–Rh1/2–O1/2	89.9(2)	89.6(2)
O1/2–Rh1/2–Cl1/2	88.01(14)	87.01(16)
Cl1/2–Rh1/2–N1/2	84.20(16)	87.97(16)
Dihedral angles		
Rh1/2–N1/2–C12/32–C11/31	5.2(12)	0.2(11)
N1/2–C12/32–C11/31–C6/26	−0.9(13)	3.1(12)
C12/32–C11/31–C6/26–O1/2	−3.5(12)	−0.9(11)
C11/31–C6/26–O1/2–Rh1/2	2.6(10)	−4.4(10)
C6/26–O1/2–Rh1/2–N1/2	0.9(6)	5.6(6)
O1/2–Rh1/2–N1/2–C12/32	−4.5(6)	−3.4(5)

5.2. Epimerization studies

The ^{1}H NMR spectrum of CpRh(pesa)Cl (**9**) at RT showed only broad signals (Scheme 9). On cooling the sample down to −60 °C in CD_2H_2 solution, the spectrum became sharp and the signals for the two diastereomers could be observed separately. The coalescence temperature T_c proved to be 283 K. The ratio at 213 K was 77:23, an assignment to the diastereomers (R_{Rh},S_C) and (S_{Rh},S_C) not being possible. The kinetic parameters for the epimerization reaction (R_{Rh}, S_C)-CpRh(pesa)Cl⇌(S_{Rh}, S_C)-CpRh(pesa)Cl were calculated on the basis of the data in Table 4 [4,21].

The half-lifes at 11.3 °C in CD_2Cl_2 are 31 ms for the forward reaction and 9.2 ms for the back reaction of the epimerization of the two diastereomers A and B. However, an assignment of A/B to (R_{Rh},S_C)/(S_{Rh},S_C) cannot be made. The reaction is faster by a factor of 2–3 than the epimerization of Cp*Rh(pesa)Cl (**1**) in CD_2Cl_2 (28 ms/6.7 ms at 21 °C) [4].

6. Supplementary material

Crystallographic data for the structural analyses have been deposited with the Cambridge Crystallographic Data Centre. For CCDC numbers see Table 1. Copies of this information may be obtained free of charge from The Director, CCDC, 12 Union Road, Cambridge, CB2 1EZ, UK (fax: +44-1223-336033; e-mail: deposit@ccdc.cam.ac.uk or www: http://www.ccdc.cam.ac.uk).

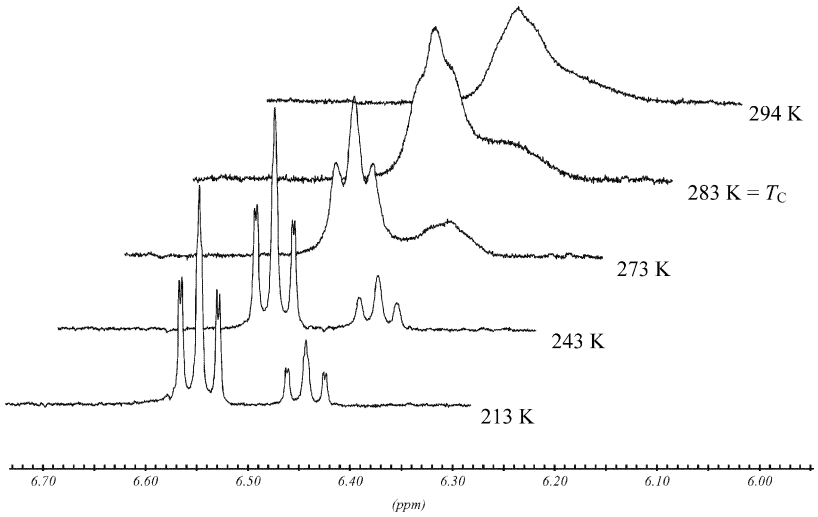

Scheme 9. ^{1}H NMR spectrum of CpRh(pesa)Cl (**9**) (400 MHz, CD_2Cl_2) at variable temperatures.

Table 4
Results of the coalescence measurements of Cp*Rh(beapy)Cl (**5**), CpRh(pesa)Cl (**9**), Cp*Rh(pesa)Cl (**1**) and Cp*Ir(pesa)Cl (**2**)

Compound	Cp*Rh(beapy)Cl (**5**)	CpRh(pesa)Cl (**9**)	Cp*Rh(pesa)Cl (**1**) (Ref. [4])	Cp*Ir(pesa)Cl (**2**) (Ref. [4])
Coalescence temperature T_c (°C)	115:1(±3)	11.3(±3)	21(±3)	−1.8(±3)
$\Delta\nu$ at T_c (extrapolated) (Hz)	16.84	39.30	52.60	39.04
Equilibrium constant (K)	1.00	0.30	0.24	0.18
Rate constant k_A (s^{-1})	15.0	22.4	24.7	13.7
Half-life τ_A (ms)	46	31	28	50
Rate constant k_B (s^{-1})	15.0	75.0	127.5	90.6
Half-life τ_B (ms)	46	9.2	6.7	8.0
Rate constant $k = k_A + k_B$ (s^{-1})	30.0	97.4	127.5	90.6
^{1}H NMR parameters	400 MHz, DMSO-D_6	400 MHz, CD_2Cl_2	400 MHz, CD_2Cl_2	400 MHz, $CDCl_3$

References

[1] H. Brunner, Adv. Organomet. Chem. 18 (1980) 151.
[2] G. Consiglio, F. Morandini, Chem. Rev. 87 (1987) 761.
[3] (a) H. Brunner, Angew. Chem. 111 (1999) 1248;
(b) H. Brunner, Angew. Chem., Int. Ed. 38 (1999) 1194.
[4] H. Brunner, A. Köllnberger, T. Burgemeister, M. Zabel, Polyhedron 19 (2000) 1519.
[5] D. Carmona, F.J. Lahoz, L.A. Oro, M.P. Lamata, F. Viguri, E. San José, Organometallics 15 (1996) 2961.
[6] D. Carmona, F.J. Lahoz, S. Elipe, L.A. Oro, Organometallics 21 (2002) 5100.
[7] W. Hoffmüller, K. Polborn, I. Krossing, H. Nöth, W. Beck, J. Organomet. Chem. 577 (1999) 93.
[8] O.E. Woisenschlager, A. Geisbauer, K. Polborn, W. Beck, J. Organomet. Chem. 599 (2000) 238.
[9] H. Brunner, Eur. J. Inorg. Chem. (2001) 905.
[10] M.L. Loza, J. Parr, A.M.Z. Slawin, Polyhedron 16 (1997) 2321.
[11] A. Köllnberger, Dissertation, University of Regensburg, Germany, 2002.
[12] H. Brunner, B. Nuber, T. Tracht, Tetrahedron: Asymmetry 9 (1998) 3763.
[13] H. Brunner, W.A. Herrmann, J. Organomet. Chem 63 (1973) 339.
[14] H.E. Smith, S.L. Cook, M.E. Warren, Jr., J. Org. Chem. 29 (1964) 2265.
[15] C. White, A. Yates, P.M. Maitlis, Inorg. Synth. 29 (1992) 228.
[16] A. Altomare, G. Cascarano, C. Giacovazzo, A. Guagliardi, J. Appl. Cryst. 27 (1993) 343.
[17] G.M. Sheldrick, SHELXL-97, University of Göttingen, Germany, 1997.
[18] C. Lecomte, Y. Dusausoy, J. Protas, J. Tirouflet, A. Dormond, J. Organomet. Chem. 73 (1974) 67.
[19] H. Brunner, Enantiomer 2 (1997) 133.
[20] H. Brunner, M. Weber, M. Zabel, T. Zwack, Angew. Chem. 115 (2003) 1903 [Angew. Chem. Int. Ed. 42 (2003) 1859].
[21] A. Jaeschke, H. Muensch, H.G. Schmid, H. Friebolin, A. Mannschreck, J. Mol. Spectrosc. 31 (1969) 14.